

Spin injection into vanadium dioxide films from a typical ferromagnetic metal, across the metal-insulator transition of the vanadium dioxide films

Kazuma Tamura^{1,a}, Teruo Kanki², Shun Shirai¹, Hidekazu Tanaka²,
Yoshio Teki³, and Eiji Shikoh^{1,a}

¹Graduate School of Engineering, Osaka City University, Osaka 558-8585, Japan

²Institute of Scientific and Industrial Research, Osaka University, Ibaraki, Osaka 567-0047, Japan

³Graduate School of Science, Osaka City University, Osaka 558-8585, Japan

^aCorresponding authors: tamura@mc.elec.eng.osaka-cu.ac.jp (K.T.), shikoh@eng.osaka-cu.ac.jp (E.S.)

A vanadium dioxide VO₂ film shows metal-insulator transition (MIT) induced by changing environmental temperature. We report the temperature dependence of electromotive force properties generated in VO₂/Ni₈₀Fe₂₀ bilayer junctions under the ferromagnetic resonance (FMR) of the Ni₈₀Fe₂₀ layer. An electromotive force generated in a VO₂/Ni₈₀Fe₂₀ bilayer junction under the FMR showed a small change across the MIT temperature of the VO₂ film, while the VO₂ film resistance drastically changed. This behavior was not only explained with the temperature dependence of the electromotive force property generated in the Ni₈₀Fe₂₀ film itself under the FMR, but also with the generated electromotive forces due to the inverse spin-Hall effect (ISHE) in the VO₂ film under the FMR of the Ni₈₀Fe₂₀ film. That is, we successfully demonstrated the spin injection from a Ni₈₀Fe₂₀ film into a VO₂ film across the MIT temperature of the VO₂ film.

To switch a pure spin current, which is a flow of spin angular momenta and a dissipation-less information propagation, by using external ways such as applying a voltage, light irradiation or heating, is an indispensable issue for future spintronic application, like spin-transistors.¹⁻³ Up to now, a Si-based spin transistor operated by applying a voltage has been demonstrated,³ and to switch a spin current through light irradiation have been challenged. Meanwhile, there are no studies for switching a spin current with an environmental temperature change, not due to the so-called spin-Seebeck effect.⁴ In this study, to switch a spin current by a temperature change, a vanadium dioxide VO₂ film which shows metal-insulator transition (MIT) with the crystal structure change induced by changing environmental temperature is focused.⁵ The MIT in VO₂ films usually occurs in the temperature range between 280 K and 350 K, depending on the film thickness,^{5,6} and a thinner VO₂ film shows an MIT at lower temperature. Recently, the spin injection into a VO₂ film from a ferrimagnetic insulator Y₃Fe₅O₁₂ (YIG) film by using the spin-pumping was achieved across the MIT temperature.⁷ However, for the practical use, to prepare high quality YIG films is needed and basically hard. Thus, in this study, the spin injection from a typical ferromagnetic metal Ni₈₀Fe₂₀ film into a VO₂ film and the controllability of the spin current in VO₂ with environmental temperature change across the MIT are tried. We report the temperature dependence of electromotive force properties generated in VO₂/Ni₈₀Fe₂₀ bilayer junctions under the ferromagnetic resonance (FMR) of the Ni₈₀Fe₂₀ layer.

Our sample structure and experimental set up are illustrated in Figures 1(a) and (b). A spin injection effect into a VO₂ film is observed as follows: in VO₂/Ni₈₀Fe₂₀ bilayer junctions, a pure spin-current, J_S , is generated in the VO₂ layer by the spin-pumping of the Ni₈₀Fe₂₀ induced by the FMR.⁸ The generated spin current is converted to a charge current, J_C , with the inverse spin-Hall effect (ISHE)⁸ in the VO₂, which is expressed as,¹⁰

$$J_C \propto \theta_{SHE} J_S \times \sigma, \quad (1)$$

where θ_{SHE} and σ are the spin-Hall angle in VO₂ films and the spin-polarization vector of the J_S , respectively. The converted J_C is detected as an electromotive force, E , via the sample resistance, R . Therefore, the E is expressed as,^{9,11}

$$E = R J_C \propto R \theta_{SHE} J_S \times \sigma. \quad (2)$$

That is, if the electromotive force due to the ISHE in VO₂ is detected under the FMR of the Ni₈₀Fe₂₀ layer, it is clear evidence of the achievement of the spin injection from a Ni₈₀Fe₂₀ layer into a VO₂ layer. We analyze the origins of the obtained electromotive forces under the FMR with some control experiments, and conclude that the spin injection

from a $\text{Ni}_{80}\text{Fe}_{20}$ film into a VO_2 film has been achieved and the spin current generation efficiency in VO_2 films by the spin pumping has been changed by the MIT.

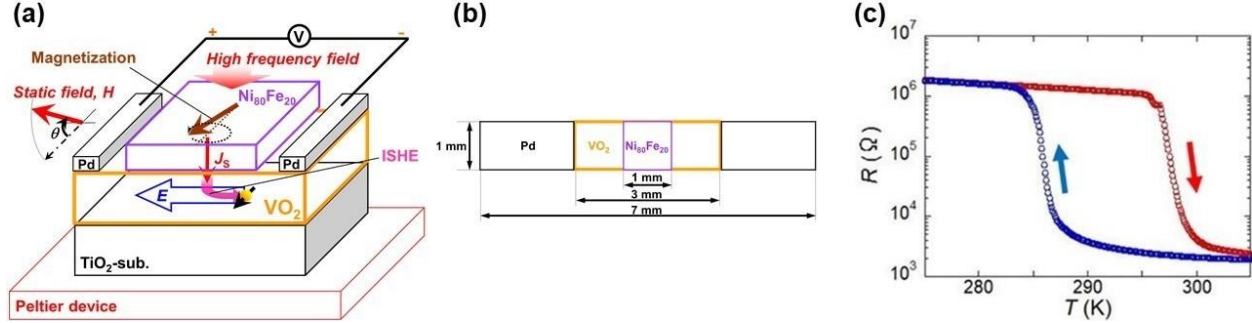


FIG. 1. (a) Bird's-eye-view and (b) top-view illustrations of our sample and orientations of external applied magnetic field H used in the experiments. J_s and E correspond to the spin current generated in a VO_2 film by the spin-pumping and the electromotive forces due to the ISHE in a VO_2 film, respectively. (c) Temperature dependence of a VO_2 film resistance.

VO_2 thin films were formed on $\text{TiO}_2(001)$ single crystal substrates using a pulsed laser deposition technique (ArF excimer: $\lambda = 193$ nm). The target employed was a sintered vanadium oxide pellet of V_2O_5 (Kojundo Chemical Lab. Co., Ltd., 99.9%). The fabrication condition of VO_2 films was at a substrate temperature of 450°C in an O_2 gas pressure of 1.0 Pa. This fabrication process is almost same as the previous result where epitaxial VO_2 films have been obtained.⁶ The VO_2 film thickness was set to be 10 nm. After the VO_2 depositions, the sample substrate was transferred to another vacuum chamber for the preparation of metal films. This transfer process and the next $\text{Ni}_{80}\text{Fe}_{20}$ deposition process were implemented as soon as possible to keep the surface state of the VO_2 films because of the surface sensitivity to the air. An electron beam (EB) deposition technique was used to deposit $\text{Ni}_{80}\text{Fe}_{20}$ (Kojundo Chemical Lab. Co., Ltd., 99.99%) to a thickness of 25 nm on the VO_2 films with a shadow mask, under a vacuum pressure of $<10^{-6}$ Pa. The deposition rate and the substrate temperature during $\text{Ni}_{80}\text{Fe}_{20}$ depositions were set to be 0.1 nm/s and an ambient temperature, respectively. Finally, palladium (Pd: Furuuchi Chemical Co., Ltd., 99.99% purity) as electrodes was deposited by EB deposition through another shadow mask, under a vacuum pressure of $<10^{-6}$ Pa. The deposition rate and the substrate temperature during Pd depositions were also set to be 0.1 nm/s and an ambient temperature, respectively.

Electrical properties were evaluated using a two-probe method with a source measure unit (Keithley Instruments, 2614B). The electrical property evaluation was implemented in a small vacuum chamber equipped with a temperature variable stage using a Peltier device. To excite FMR in $\text{Ni}_{80}\text{Fe}_{20}$ for investigation of the spin injection effect into VO_2 films, a coplanar waveguide connected to a vector network analyzer (VNA: KEYSIGHT Technology, N5221A) and a couple of electromagnets were used. A nano-voltmeter (Keithley Instruments, 2182A) to detect electromotive forces from the samples was used. This spin-pumping experiment system also equips with another Peltier device under the sample mount position. Leading wires for detecting the output voltage properties were directly attached at the two Pd electrodes of samples with silver paste.

Figure 1(c) shows a temperature dependence of resistance of a VO_2 film. The sample temperature was changed with a rate of 2 K/min, monitoring with a thermocouple. The VO_2 film resistance changes by three orders of magnitude and shows a hysteresis in this temperature range, reflecting the typical MIT of VO_2 films.^{5,6} Moreover, the VO_2 resistance is steeply changed which is a typical evidence that the VO_2 film is almost epitaxially grown.⁶

The inset in Figure 2(a) shows an FMR spectrum for a $\text{VO}_2/\text{Ni}_{80}\text{Fe}_{20}$ bilayer junction at 300 K, where an external magnetic field orientation angle to the sample film plane, θ , is 0° and the frequency of the high frequency electrical current, f , is 5 GHz. The FMR field of the $\text{Ni}_{80}\text{Fe}_{20}$ film, H_{FMR} , is 325 Oe, and the saturation magnetization of the $\text{Ni}_{80}\text{Fe}_{20}$ film, M_S , is estimated to be 671 G under the FMR conditions in the case of the in-plane field:¹²

$$\frac{\omega}{\gamma} = \sqrt{H_{\text{FMR}}(H_{\text{FMR}} + 4\pi M_S)}, \quad (3)$$

where ω and γ are the angular frequency $2\pi f$ and the gyromagnetic ratio of $1.86 \times 10^7 \text{ G}^{-1}\text{s}^{-1}$ of $\text{Ni}_{80}\text{Fe}_{20}$, respectively. The main panel of Fig. 2(a) shows output voltage properties of the same $\text{VO}_2/\text{Ni}_{80}\text{Fe}_{20}$ bilayer junction under the FMR of the $\text{Ni}_{80}\text{Fe}_{20}$ layer at 300 K. Clear output voltage properties have been observed and the voltage sign has been inverted at the magnetization reversal of the $\text{Ni}_{80}\text{Fe}_{20}$ layer. This voltage sign inversion associated with the magnetization reversal in $\text{Ni}_{80}\text{Fe}_{20}$ is a characteristic of the typical ISHE.^{9,13,14} The solid lines in Fig. 2(a) are the curve fits obtained using the following equation:^{9,14}

$$V(H) = V_{Sym} \frac{\Gamma^2}{(H - H_{FMR})^2 + \Gamma^2} + V_{Asym} \frac{-2\Gamma(H - H_{FMR})}{(H - H_{FMR})^2 + \Gamma^2}, \quad (4)$$

where H is an external static magnetic field and Γ denotes the damping constant (18.0 Oe in this study). The first and second terms in the eq. (4) correspond to the symmetry term to H (e.g. the ISHE) and the asymmetry term to H (e.g. the anomalous Hall effect and other effects showing the same asymmetric voltage behavior relative to the H , like parasitic capacitances), respectively. V_{Sym} and V_{Asym} correspond to the coefficients of the first and second terms in eq. (4), respectively. On the other hand, Fig. 2(b) shows the output voltage properties of a $\text{Cu}/\text{Ni}_{80}\text{Fe}_{20}$ bilayer junction under the FMR of the $\text{Ni}_{80}\text{Fe}_{20}$ layer at 300 K. No clear output voltages were observed at the H_{FMR} of the $\text{Ni}_{80}\text{Fe}_{20}$ layer. Since Cu has small spin orbit interaction to generate the ISHE, this behavior is reasonable. This suggests the observed electromotive forces in the $\text{VO}_2/\text{Ni}_{80}\text{Fe}_{20}$ bilayer junctions under the FMR of the $\text{Ni}_{80}\text{Fe}_{20}$ layer are mainly due to the ISHE in VO_2 films. Also, we can say that the electromotive force generated in the $\text{Ni}_{80}\text{Fe}_{20}$ layer itself under the FMR is shunted in the Cu layer. This similar shunting effect for the samples with VO_2 can also be taken into account to explain the results.

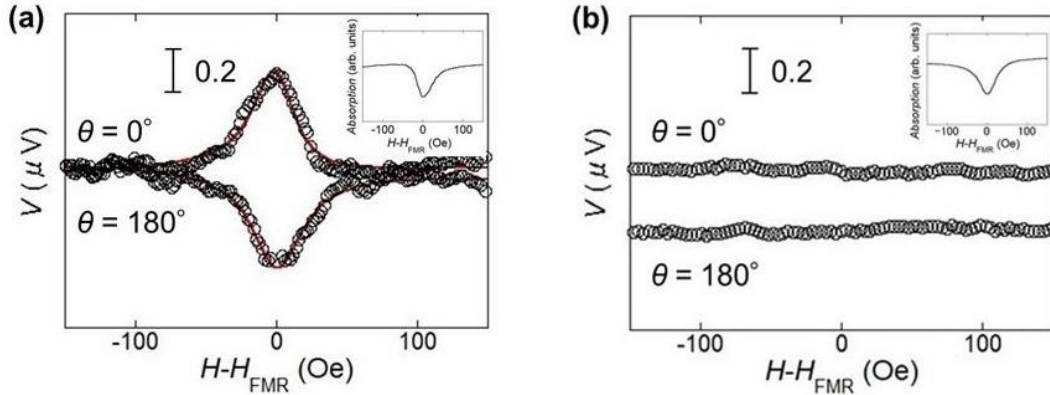


FIG. 2. (a) Output voltage properties of a $\text{VO}_2/\text{Ni}_{80}\text{Fe}_{20}$ bilayer junction under the FMR of the $\text{Ni}_{80}\text{Fe}_{20}$ layer at 300 K. The inset shows the FMR spectrum for the bilayer junction at 300 K, and at the θ of 0° . (b) Output voltage properties of a $\text{Cu}/\text{Ni}_{80}\text{Fe}_{20}$ bilayer junction under the FMR of the $\text{Ni}_{80}\text{Fe}_{20}$ layer at 300 K. The inset shows the FMR spectrum for the bilayer junction at 300 K, and at the θ of 0° .

Figure 3 shows temperature dependences of the V_{Sym} of a $\text{VO}_2/\text{Ni}_{80}\text{Fe}_{20}$ bilayer sample (circles) and the sample resistance (a solid line). As the VO_2 film changed from an insulator to a metal, the V_{Sym} became slightly small. This behavior is not only be explained with the electromotive force property generated in the $\text{Ni}_{80}\text{Fe}_{20}$ film itself under the FMR¹⁵ since the resistance of VO_2 films is drastically changed across the MIT and the ferromagnetic transition temperature is much higher than the temperature range in this study. Thus, to explain the small change of the V_{Sym} against the temperature, the θ_{SHE} and the injected J_S into VO_2 films must be changed by controlling the environmental temperature under the relationship expressed as the eq. (2). This is reasonable because the crystal structure of VO_2 is changed across the MIT, that is, the electronic properties in VO_2 films are drastically changed across the MIT. The electromotive force generated in the interface between the VO_2 and $\text{Ni}_{80}\text{Fe}_{20}$ films in the $\text{VO}_2/\text{Ni}_{80}\text{Fe}_{20}$ junctions may be considered by using, for example, other MIT materials⁵ and it is an interesting study, whereas this is also excluded by the shunting effect in the VO_2 film. That is, the ISHE in VO_2 films is dominant as origins of observed electromotive forces in the $\text{VO}_2/\text{Ni}_{80}\text{Fe}_{20}$ junctions under the FMR. Thus, we concluded that the spin injection into VO_2 films was achieved by the spin-pumping using a $\text{Ni}_{80}\text{Fe}_{20}$ film.

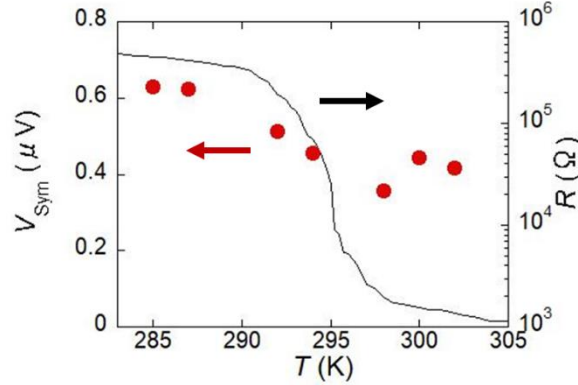


FIG. 3. Temperature dependences of the electromotive forces generated in a VO₂/Ni₈₀Fe₂₀ bilayer junction under the FMR of the Ni₈₀Fe₂₀ film (circles) and the sample resistance (a solid line).

Finally, in order to investigate the spin current generation efficiency by the spin pumping, we focused on the real part of the spin mixing conductance, $g_r^{\uparrow\downarrow}$, which represents the parameter to determine the spin pumping efficiency at the interface between the Ni₈₀Fe₂₀ and the VO₂ layers. The $g_r^{\uparrow\downarrow}$ is expressed as,¹⁶

$$g_r^{\uparrow\downarrow} = \frac{4\pi M_S d_F}{g\mu_B} (\alpha - \alpha_0), \quad (5)$$

where g , μ_B , d_F , α , and α_0 are the Landé g-factor, the Bohr magneton, the thickness of the Ni₈₀Fe₂₀ layer, the Gilbert damping constant, and the intrinsic Gilbert damping constant of the Ni₈₀Fe₂₀, respectively. The $g_r^{\uparrow\downarrow}$ depends on the α . In other words, the spin current generation efficiency depends on the α . Figure 4(a) shows a frequency dependence of the half width at half maximum resonance linewidth, ΔH , for a VO₂/Ni₈₀Fe₂₀ bilayer junction in the temperature range across the MIT. The α is obtained using the following equation:¹⁷

$$\Delta H = \Delta H_0 + \frac{2\pi\alpha}{|\gamma|} f, \quad (6)$$

where ΔH_0 is the frequency independent ΔH . Fig. 4(b) shows temperature dependence of the α of a VO₂/Ni₈₀Fe₂₀ bilayer junction (red circles) and a Ni₈₀Fe₂₀ single layer sample (black circles). The α of a VO₂/Ni₈₀Fe₂₀ bilayer junction increased at a higher temperature, while the α of a Ni₈₀Fe₂₀ single layer sample is almost constant in this temperature range. Since the $g_r^{\uparrow\downarrow}$ depends on the α , we have concluded that the spin current generation efficiency by the spin pumping is affected by the MIT. The temperature dependence of the α of the VO₂/Ni₈₀Fe₂₀ bilayer junction is also an evidence of the spin injection effect from the Ni₈₀Fe₂₀ layer into the VO₂ layer.

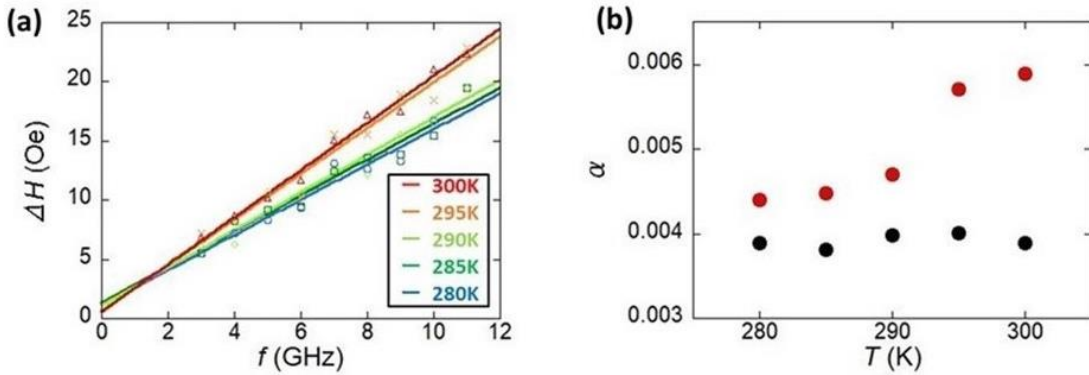


FIG. 4. (a) Frequency dependence of the half width at half maximum resonance linewidth, ΔH , for a VO₂/Ni₈₀Fe₂₀ bilayer junction in the temperature range of the MIT. (b) Temperature dependences of the Gilbert damping constant, α , of a VO₂/Ni₈₀Fe₂₀ bilayer junction and a Ni₈₀Fe₂₀ single layer sample.

In summary, we reported the temperature dependence of electromotive force properties generated in VO₂/Ni₈₀Fe₂₀ bilayer junctions under the FMR of the Ni₈₀Fe₂₀ layer. The detected electromotive forces in the bilayer junctions under the FMR showed a small change in the temperature range, while the resistance VO₂ films was drastically changed across the MIT. This behavior was not only explained with the temperature dependence of the electromotive force property generated in the Ni₈₀Fe₂₀ film itself under the FMR. The ISHE in VO₂ films was the dominant origin of the generated electromotive forces in the VO₂/Ni₈₀Fe₂₀ bilayer junctions under the FMR, that is, we achieved the spin injection from Ni₈₀Fe₂₀ into a MIT compound, VO₂. Additionally, the Gilbert damping constant increased at higher temperatures, that is, the spin current generation efficiency by the spin pumping from a Ni₈₀Fe₂₀ film into a VO₂ film was changed by the MIT.

This research was partly supported by a Grant-in-Aid from the Japan Society for the Promotion of Science (JSPS) for Scientific Research (B) (26286039 (to E. S. and T. K.)), by the Cooperative Research Program of "NJRC Mater. & Dev.," (to E. S., T. K. and H. T.) and by the OCU Strategic Research Grant 2018 for top priority researches (to E. S.).

The data that support the findings of this study are available from the corresponding author upon reasonable request.

- ¹ S. Datta and B. Das, *Appl. Phys. Lett.* **56**, 665 (1990).
- ² S. Sugahara, and M. Tanaka, *Appl. Phys. Lett.* **84**, 2307 (2004).
- ³ T. Tahara, H. Koike, M. Kameno, T. Sasaki, Y. Ando, K. Tanaka, S. Miwa, Y. Suzuki, and M. Shiraishi, *Appl. Phys. Exp.* **8**, 113004 (2015).
- ⁴ K. Uchida, S. Takahashi, K. Harii, J. Ieda, W. Koshibae, K. Ando, S. Maekawa, and E. Saitoh, *Nature* **455**, 778 (2008).
- ⁵ H. Takami, T. Kanki, S. Ueda, K. Kobayashi, and H. Tanaka, *Appl. Phys. Exp.* **3**, 063201 (2010).
- ⁶ Y. Tsuji, T. Kanki, Y. Murakami, and H. Tanaka, *Appl. Phys. Exp.* **12**, 025003 (2019).
- ⁷ T.S. Safi, P. Zhang, Y. Fan, Z. Guo, J. Han, E.R. Rosenberg, C. Ross, Y. Tserkovnyak, and L. Liu, *Nature. Commun.*, **11**, 476 (2020).
- ⁸ S. Mizukami, Y. Ando, and T. Miyazaki, *Phys. Rev. B* **66**, 104413 (2002).
- ⁹ E. Saitoh, M. Ueda, H. Miyajima, and G. Tatara, *Appl. Phys. Lett.* **88**, 182509 (2006).
- ¹⁰ K. Ando, Y. Kajiwara, S. Takahashi, S. Maekawa, K. Takemoto, M. Takatsu, and E. Saitoh, *Phys. Rev. B* **78**, 014413 (2008).
- ¹¹ K. Ando, S. Takahashi, J. Ieda, Y. Kajiwara, H. Nakayama, T. Yoshino, K. Harii, Y. Fujikawa, M. Matsuo, S. Maekawa, and E. Saitoh, *J. Appl. Phys.* **109**, 103913 (2011).
- ¹² C. Kittel, *Phys. Rev.* **73**, 155 (1948).
- ¹³ K. Ando and E. Saitoh, *J. Appl. Phys.* **108**, 113925 (2010).
- ¹⁴ E. Shikoh, K. Ando, K. Kubo, E. Saitoh, T. Shinjo, and M. Shiraishi, *Phys. Rev. Lett.* **110**, 127201 (2013).
- ¹⁵ A. Tsukahara, Y. Ando, Y. Kitamura, H. Emoto, E. Shikoh, M. P. Delmo, T. Shinjo, and M. Shiraishi, *Phys. Rev. B* **89**, 235317 (2014).
- ¹⁶ Y. Tserkovnyak, A. Brataas, G.E.W. Bauer and B.I. Halperin, *Rev. Mod. Phys.* **77**, 1375 (2005).
- ¹⁷ T. Nan, S. Emori, C. T. Boone, X. Wang, T. M. Oxholm, J. G. Jones, B. M. Howe, G. J. Brown, and N. X. Sun, *Phys. Rev. B* **91**, 214416 (2015).